Liu *et al. Journal of Biological Engineering* (2025) 19:40
https://doi.org/10.1186/s13036-025-00510-2

Journal of Biological Engineering

RESEARCH

Open Access

Engineered supercooling systems for enhanced long-term preservation of large-volume red blood cells in commercial blood bags

Qi Liu[1†], Shichun Wang[1†], Jie Yan[1], Ronghua Diao[1], Haishui Huang[3,4], Feng Xu[3,4*] and Chunyan Yao[1,2*]

Abstract

Reducing cell metabolism by lowering the storage temperature is an important method to improve the quality of stored RBCs and prolong the stored shelf life of RBCs. Traditional cryopreservation suffers from limitations such as tedious cytotoxic cryoprotectants (CPA) loading, unloading and ice-induced damage. Storage around 2–6 °C is an alternative method but only works for a short period due to significant storage lesions at this high storage temperature. We developed an improved supercooling preservation system for large-volume (100 ml) RBC suspensions in commercial polyvinylchloride (PVC) blood bags by minimizing favorable sites of ice nucleation and maintaining precise thermal control at –8 °C. This engineered protocol significantly reduces hemolysis, metabolic degradation, and oxidative stress while preserving RBC membrane integrity and functionality for up to 63 days. In vivo transfusion studies in New Zealand white rabbits demonstrate that supercooling-preserved RBCs achieve higher post-transfusion recovery rates, outperforming conventional storage methods. Our scalable and cost-effective supercooling system address critical needs for improving the quality of stored RBCs by achieving ice-free preservation, which representing a significant breakthrough in transfusion medicine.

Keywords Supercooling Preservation, Red Blood Cells, Blood Bags, Metabolic Stability, Oxidative Stress

Introduction

Red blood cell (RBC) transfusion is a cornerstone of modern medicine, vital for treating acute hemorrhage, chronic anemia, and supporting perioperative care [1–3]. With the advancement of clinical treatment technology and the intensification of population aging, the quality of stored RBCs becomes particularly important in the use of limited blood resources. RBCs undergo biochemical and physical changes during storage known as "storage lesions" [4–6]. Over the years, additive solutions have been continuously optimized for reducing storage lesions, evolving from acidic formulations to the development of modern alkaline additive solutions. These improvements better sustain RBC metabolism, progressively extending stored RBCs shelf life—up to 49 days,

†Qi Liu and Shichun Wang contributed equally to this work.

*Correspondence:
Feng Xu
fengxu@mail.xjtu.edu.cn
Chunyan Yao
yaochunyan@tmmu.edu.cn
[1] Department of Blood Transfusion, First Affiliated Hospital, Third Military Medical University (Army Medical University), Chongqing 400038, P.R. China
[2] State Key Laboratory of Trauma and Chemical Poisoning, Third Military Medical University, Chongqing 400038, P.R. China
[3] The Key Laboratory of Biomedical Information Engineering of Ministry of Education, School of Life Science and Technology, Xi'an Jiaotong University, Xi'an 710049, P.R. China
[4] Bioinspired Engineering and Biomechanics Center (BEBC), Xi'an Jiaotong University, Xi'an 710049, P.R. China

e.g., in PAGGS-M/Adsol solutions at 2–6 °C [7–9]. On the other hand, storage temperature is a critical factor in RBC metabolism, as lower temperatures slow cellular metabolic activity [10, 11]. Thus, establishing a novel low-temperature storage method to solve RBC storage lesion has remained a key focus for blood bank.

Storage around 2–6 °C is an alternative low-temperature storage method. But it ensures high transfusion efficiency only for a short period due to significant storage lesions at this high storage temperature. These storage lesions include reduced levels of adenosine triphosphate (ATP) and 2,3-diphosphoglycerate (2,3-DPG), increased oxidative stress, and membrane protein alterations, all of which compromise RBC viability and efficacy [12–16]. Clinical studies have linked the transfusion of older RBC units (> 2 weeks, 2–6 °C) to elevated risks of postoperative complications, infections, and higher mortality rates [17]. While cryopreservation at -80 °C extends stored RBC shelf life beyond a decade using high concentrations of glycerol (> 20%). However, the challenges posed by this method remain unsolved [6]. The addition and removal of glycerol cause osmotic stress and hemolysis, and the deglycerolization process is laborious and time-consuming, delaying emergency transfusions [18, 19]. Additionally, cryopreservation risks cryoinjuries such as intracellular ice formation and recrystallization, further reducing RBC viability [20, 21]. Alternative methods like freeze-drying, though promising for room-temperature storage, still expose RBCs to ice-induced damage, resulting in reduced viability [22]. One recent advance is the preservation of RBCs at -8.0 °C for an impressive 70 days without freezing by adding a low concentration of glycerol combined with PEG-400 to reduce the freezing point [23]. With this preservation method, approximately 95% of RBCs survive post-rewarming. However, given the tedious rewarming and washing processes and very small storage volume (5 ml), its clinical practicality remains limited.

In pursuit of evolving translational solutions, researchers have strived to refine pRBCs storage methods to ensure longevity and clinical efficacy [13, 24–31]. Supercooling, by definition, which maintains substances below the freezing point without solidification (between -20 °C and -3 °C), has recently emerged as a potential game-changer for preserving cells, tissues, and organs [32–39]. This method minimizes ice-mediated damage and metabolic activity, preserving cell integrity over extended periods. Previous studies have successfully supercooled small volumes (1 ml) of RBC suspensions in polystyrene rigid tubes for up to 100 days using paraffin oil sealing, achieving minimal hemolysis and high hemoglobin recovery rates [40]. However, supercooling preservation is still limited to small-volume storage and is insufficient to meet the requirements for large-volume RBC preservation in clinical settings. So far, it is still difficult to maintain supercooled water unfrozen, especially for low temperature (< − 10 °C), large volume (> 1 ml), and long period (> 1 week). Because each of these increases the possibility of ice nucleation and water freezing [33, 40–42].

Currently, maintaining adequate RBC supplies in blood banks relies on advanced storage systems utilizing commercial blood bags constructed from flexible, sterile, gas-permeable PVC materials [43–46]. These commercial blood bags preserve cellular integrity through three key mechanisms: 1) minimizing mechanical hemolysis via compliant and super smooth surfaces, 2) facilitating essential gas exchange through selective membrane permeability, and 3) maintaining metabolic homeostasis and reducing oxidative stress through optimal additive solutions. This multimodal preservation approach significantly enhances transfusion safety while complying with international blood banking gold standards (AABB guidelines) [3]. However, scaling supercooling preservation techniques to clinically large-volume at physiological hematocrit levels presents below technical challenges. Increased ice nucleation propensity governed by the classical nucleation theory relationship, where larger volumes and extended storage durations exponentially raise crystallization probability [20, 39]. In addition, unlike rigid containers (e.g., glass or polystyrene tubes), the flexible PVC blood bags deform easily under external forces or thermal fluctuations, disrupting the paraffin oil seal designed to inhibit ice nucleation at the liquid–air interface. This deformation causes the oil layer to shift or mix with the RBC suspension [47–49]. This thermodynamic-structural paradox creates critical barriers to implementing supercooling preservation in standard blood banking operations, necessitating fundamental material science innovations coupled with advanced thermal control strategies.

In this study, we present an innovative supercooling preservation protocol tailored for large-volume (100 ml) RBC suspensions stored in commercial PVC blood bags. By engineering a system that minimizes nucleation sites through paraffin oil sealing and stabilizes storage conditions with precise thermal control, we achieved successful supercooling of RBCs at -8℃ for up to 63 days under meet the Food and Drug Administration (FDA) standards condition. Compared to traditional supercooling preservation methods, we can now increase the RBC storage volume by up to 100 times, maintaining a standard hematocrit level, all while employing a standard blood bag as the storage container. Our protocol significantly reduces hemolysis, metabolic degradation, and oxidative stress while maintaining RBC membrane integrity and

functionality. In vivo transfusion studies in New Zealand white rabbits demonstrated superior post-transfusion recovery rates compared to conventionally stored RBCs. This scalable and cost-effective supercooling system in commercial PVC blood bags is compatible with existing blood banking infrastructure, offering a robust and clinically relevant solution poised to transform transfusion medicine by extending RBC shelf life and enhancing transfusion outcomes.

Results

Optimization of supercooling preservation conditions enhances RBC stability

Supercooling preservation relies on preventing heterogeneous nucleation at the liquid–air interface, typically achieved using an immiscible oil phase [39–42]. While this strategy has proven effective in rigid round-bottomed polystyrene tubes, which maintain the stability of the oil–water interface, its application in flexible PVC blood bags presents significant challenges. Flexible blood bags are prone to deformation under external forces, potentially disrupting the oil layer and initiating ice nucleation, thereby compromising the supercooled state. To address this issue, we adhered the outer surface of the PVC blood bags to a rigid baseplate using double-sided tape, thereby preventing deformation and ensuring the integrity of the oil seal during storage. This engineering modification is crucial for maintaining a stable supercooled environment in flexible blood bags.

The maintenance of metastable supercooled states in RBC suspensions in PVC blood bags is critically influenced by multiple factors. To develop an optimized supercooling protocol for RBC in PVC blood bags, an orthogonal experimental design (Table 1) was implemented to systematically evaluate six critical factors at each three levels: 1) paraffin oil sealing volume, 2) storage temperature, 3) RBC suspension volume, 4) cooling rate, 5) blood bag placement angle, and 6) baseplate material. The liquid–air interface is thermodynamically conducive to heterogeneous ice nucleation due to surface tension [48]; therefore, we minimized potential ice nucleation sites by sealing the blood bags with paraffin oil. Additionally, ice formation during the supercooling process is a stochastic phenomenon influenced by several factors, including RBC volume, storage temperature, and cooling rate. The likelihood of ice nucleation within the supercooled volume increases with larger RBC volumes, faster cooling rates, and lower storage temperatures. Furthermore, the blood bag placement angle directly modulates the RBC suspension/air interfacial area and wrap-baseplate material selection significantly impacts thermal exchange dynamics (Fig. S1).

The orthogonal experimental design systematically assessed three levels for each of the six factors, reducing the complexity from 729 potential combinations to 18 experimental setups. Each setup was evaluated based on freezing frequency, defined as the ratio of frozen samples to total samples, to determine supercooling stability. Analysis of variance revealed that storage temperature (Vk = 0.1333) and RBC volume (Vk = 0.1282) were the most significant factors influencing freezing frequency, followed by placement angle (Vk = 0.0971) (Table 2). Cooling rate, baseplate material, and sealing oil volume also impacted freezing frequency but to a lesser extent. Under the optimal conditions identified, *i.e.*, storing 100 ml of RBC suspensions sealed with 8 ml of paraffin oil, cooled slowly to -8.0 °C, and maintained vertically in a monitoring refrigerator, we achieved the lowest freezing frequency, indicating enhanced supercooling stability (Fig. S2).

The engineered steps for the supercooling preservation of RBC in commercial blood bags are illustrated in Fig. 1A. Supercooled state stability relies on two parameters, *i.e.*, slower cooling rate to the supercooling temperature and minimal temperature fluctuations during storage [33, 50–55]. However, During the blood storage process, temperature fluctuations within the blood storage refrigerator are inevitable due to its operational mode of the cooling and heating cycles. We further analyzed the impact of various thermally conductive materials (copper, glass, styrofoam) as baseplates for supercooled storage. During cooling, we recorded temperature changes at the bottom, middle, and top of the blood bags. Copper takes about 130 min, glass 150 min, and styrofoam 360 min to reach the target temperature of -8.0 °C (Fig. 1B-D). The refrigerator's cyclical freezing compressor activity causes temperature oscillations every 30 min, with fluctuations around 2.3 °C. Different wraps of the blood bag modify

Table 1 Experimental factors with three levels

Level	Placement angle	Baseplate materials	Cooling rate	Storage volume	Storage temperature	Sealing oil volume
I	flat	styrofoam	rapid	100 ml	-12 °C	8 ml
II	tilt	glass	middle	150 ml	-10 °C	14 ml
III	vertical	copper plate	slow	200 ml	-8 °C	20 ml

Table 2 Orthogonal experimental design results and factor significance

Test No	Placement angle	Baseplate materials	Cooling rate	Storage volume	Storage temperature	Sealing oil volume	Freezing frequency (F_f)	Transformed F_f
1	$tilt_{-II}$	$glass_{-II}$	$rapid_{-I}$	150 ml_{-II}	-10℃$_{-II}$	20 ml_{-III}	**80%**	**1.11**
2	$flat_{-I}$	$copper_{-III}$	$slow_{-III}$	150 ml_{-II}	-10℃$_{-II}$	14 ml_{-II}	**70%**	**0.99**
3	$vertical_{-III}$	$styrofoam_{-I}$	$rapid_{-I}$	200 ml_{-III}	-10℃$_{-II}$	20 ml_{-III}	**70%**	**0.99**
4	$vertical_{-III}$	$styrofoam_{-I}$	$slow_{-III}$	100 ml_{-I}	-10℃$_{-II}$	14 ml_{-II}	**30%**	**0.58**
5	$tilt_{-II}$	$styrofoam_{-I}$	$middle_{-II}$	200 ml_{-III}	-8℃$_{-III}$	14 ml_{-II}	**50%**	**0.79**
6	$flat_{-I}$	$glass_{-II}$	$rapid_{-I}$	200 ml_{-III}	-8℃$_{-III}$	14 ml_{-II}	**90%**	**1.25**
7	$flat_{-I}$	$styrofoam_{-I}$	$middle_{-II}$	150 ml_{-II}	-12℃$_{-I}$	20 ml_{-III}	**80%**	**1.11**
8	$tilt_{-II}$	$styrofoam_{-I}$	$slow_{-III}$	150 ml_{-II}	-8℃$_{-III}$	8 ml_{-I}	**30%**	**0.58**
9	$flat_{-I}$	$glass_{-II}$	$slow_{-III}$	100 ml_{-I}	-8℃$_{-III}$	20 ml_{-III}	**40%**	**0.68**
10	$vertical_{-III}$	$copper_{-III}$	$middle_{-II}$	100 ml_{-I}	-8℃$_{-III}$	20 ml_{-III}	**20%**	**0.46**
11	$tilt_{-II}$	$copper_{-III}$	$rapid_{-I}$	100 ml_{-I}	-12℃$_{-I}$	14 ml_{-II}	**70%**	**0.99**
12	$tilt_{-II}$	$glass_{-II}$	$middle_{-II}$	100 ml_{-I}	-10℃$_{-II}$	8 ml_{-I}	**50%**	**0.79**
13	$vertical_{-III}$	$glass_{-II}$	$slow_{-III}$	200 ml_{-III}	-12℃$_{-I}$	8 ml_{-I}	**80%**	**1.11**
14	$vertical_{-III}$	$copper_{-III}$	$rapid_{-I}$	150 ml_{-II}	-8℃$_{-III}$	8 ml_{-I}	**30%**	**0.58**
15	$flat_{-I}$	$styrofoam_{-I}$	$rapid_{-I}$	100 ml_{-I}	-12℃$_{-I}$	8 ml_{-I}	**70%**	**0.99**
16	$vertical_{-III}$	$glass_{-II}$	$middle_{-II}$	150 ml_{-II}	-12℃$_{-I}$	14 ml_{-II}	**60%**	**0.89**
17	$flat_{-I}$	$copper_{-III}$	$middle_{-II}$	200 ml_{-III}	-10℃$_{-II}$	8 ml_{-I}	**80%**	**1.11**
18	$tilt_{-II}$	$copper_{-III}$	$slow_{-III}$	200 ml_{-III}	-12℃$_{-I}$	20 ml_{-III}	**70%**	**0.99**
I	**6.13**	**5.04**	**5.91**	**4.49**	**6.08**	**5.16**		
II	**5.25**	**5.83**	**5.15**	**5.26**	**5.57**	**5.49**		
III	**4.61**	**5.12**	**4.93**	**6.24**	**4.34**	**5.34**		
S_k	**0.1941**	**0.0630**	**0.0881**	**0.2564**	**0.2667**	**0.0091**		
V_k	**0.0971**	**0.0315**	**0.0441**	**0.1282**	**0.1333**	**0.0046**		

I, II, and III are the summations of the transformed freezing frequencies from the tests that involve levels I, II, and III, respectively. The smallest values among I, II, and III indicate the level with the lowest freezing frequency for the sample. S_k is the sum of the squares, which corresponds to the variation in the variety mean. V_k is the mean square and is defined as $V_k = S_k / f_k$, where f_k is the number of degrees of freedom. V_k represents the significance of each factor's main effect, and a higher V_k value signifies a greater significance for the freezing frequency. By our analysis, the best combination is slow cooling, styrofoam baseplate, 8 ml of sealing oil, -8℃, vertical orientation and 100 ml storage volume

N = 10 (Each condition was tested once with 10 replicate samples)

F_f: Freezing frequency

Transformed $F_f = \arcsin(\sqrt{freezing\ frequency})$

$S_k = (I^2 + II^2 + III^2) / 6 - (I + II + III)^2 / 18;\ V_k = S_k / 2$

temperature fluctuations: 2.0 °C for wrap-copper, 0.7 °C for wrap-glass, and 0.3 °C for wrap-styrofoam (Fig. 1E-F). We also assessed freezing frequencies for blood cells at various subzero storage temperatures (-8.0 to -13.0 °C) preserved for 2 days. At -10.0 °C, the freezing frequency is 90% for wrap-copper, 60% for wrap-glass, and 30% for wrap-styrofoam. The results show that the use of styrofoam as the baseplate material supported a slower cooling rate and minimized temperature fluctuations during long-term storage, further reducing the likelihood of ice nucleation (Fig. 1G). Time-dependent temperature profiles at the bottom of PVC blood bags during the supercooling process for wrap-styrofoam (–8 °C target), data were recorded at 1-min intervals over 360 min, showing an initial rapid cooling phase (0–60 min: average rate = 0.10 °C/min) followed by a stabilized phase (60–360 min: average rate = 0.046 °C/min). Final equilibrium temperature reached –8.0 °C, with no ice nucleation observed (Fig. 1H). Our results further confirm that maintaining a slow cooling rate and minimizing temperature fluctuations were critical in sustaining the supercooled state as evidenced by the superior performance of styrofoam-wrapped blood bags compared to those wrapped with copper or glass (Fig. 1I, S3-4).

These findings demonstrate that precise control of cooling parameters and sealing methods, combined with structural reinforcement of the blood bags, are essential for maintaining the supercooled state in large-volume RBC suspensions in commercial blood bags. The optimized protocol not only minimizes ice

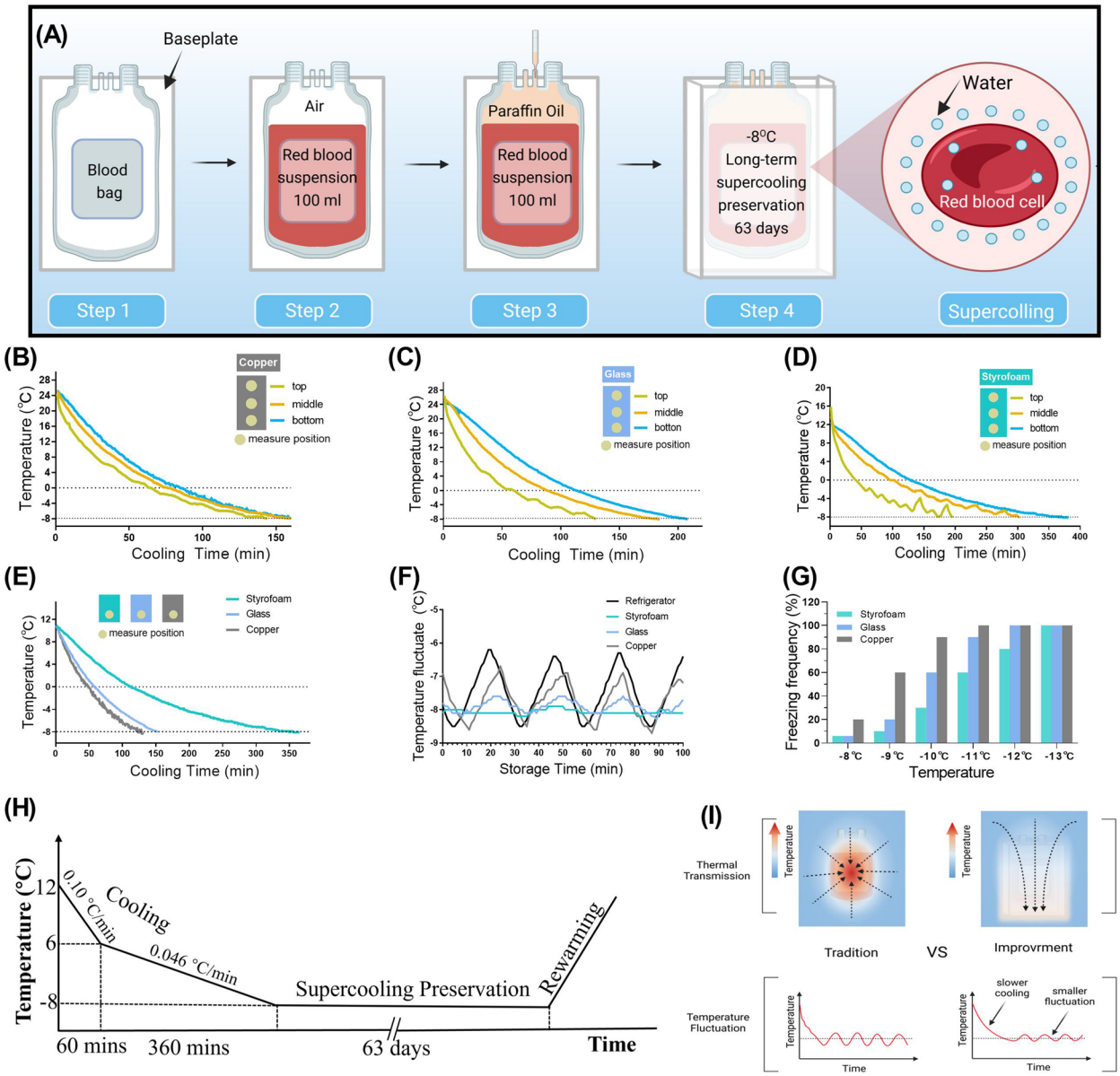

Fig. 1 Optimization of supercooling preservation conditions. **A** Experimental steps for engineered supercooling preservation. **B-D** Temperature profiles during cooling for different baseplate materials, the temperature recorded at blood bag top, middle and bottom position with a wrap-copper **B**), glass **C**), styrofoam **D**) during the whole cooling process. **E** Effect of different thermal conductivity material as wrap-baseplate on the cooling rate analysis. **F** Temperature fluctuations and stability analysis for copper, glass, and styrofoam wraps. **G** Freezing frequency across various subzero temperatures. Freezing frequencies of 100 ml pRBCs suspensions sealed by 8 ml paraffin oil with different wrap-baseplate, stored under different temperatures (-8, -9, -10, -11, -12 and -13 °C) for 2 days, per group tested once with 10 replicate samples ($N = 10$). **H** Temperature Profile During Supercooling Preservation. **I** Illustration of temperature heat transfer for supercooling preservation. slower cooling rate to the supercooling temperature and minimal temperature fluctuations during storage contribute to supercooling preservation

nucleation but also ensures scalability and reliability, making it suitable for clinical applications. By addressing the inherent challenges associated with flexible blood bags, our engineered supercooling preservation system significantly enhances RBC stability, laying the groundwork for improved long-term storage solutions in transfusion medicine.

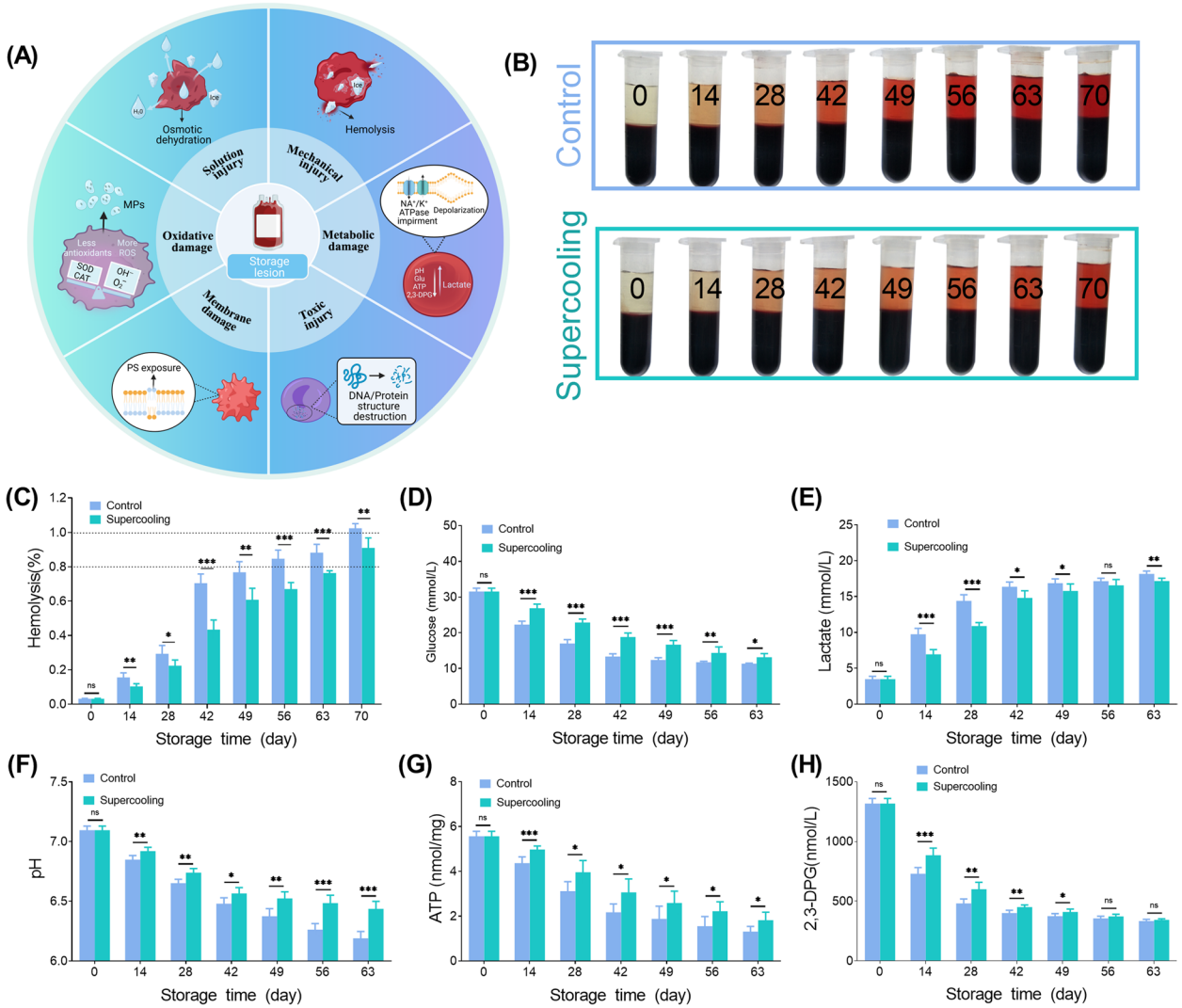

Fig. 2 In vitro analysis hemolysis and metabolic degradation of RBC. **A** Mechanism of RBC storage lesion, including metabolic damage, oxidative damage, membrane damage, mechanical injury, solution injury, toxic injury. **B** Visual inspection of RBC supernatants post-centrifugation. Photos of RBC supernatant after centrifugation at 0, 14, 28, 42, 49, 56, 63, and 70 days. **C** Mean values of hemolysis over 63 days. **D-H** Metabolic parameters: glucose, lactate, pH, ATP, and 2,3-DPG levels. Mean values of glucose **D**), lactate **E**), pH **F**), ATP **G**), 2,3-DPG **H**) in RBC samples at 0, 14, 28, 42, 49, 56, and 63 days. Control (blue) and supercooled (green). Data are shown as the mean ± SD from six biological replicates ($n = 6$). independent samples t-test, $^{*}p < 0.05$; $^{***}p < 0.001$; ns, nonsignificant

Supercooling preservation minimizes hemolysis and metabolic degradation of RBC

To evaluate the efficacy of supercooling preservation in maintaining RBC integrity and metabolic stability, we conducted comprehensive in vitro analyses over a 63-day storage period (Fig. 2A, S5). Hemolysis is a critical indicator of RBC preservation quality, with the current regulatory threshold set at < 0.8% [56]. Hemolysis was assessed by measuring free hemoglobin (F-Hb) levels in the supernatant post-centrifugation. Visual inspection of RBC supernatants (Fig. 2B) corroborated these findings, with supercooling-preserved samples displaying less discoloration, indicative of reduced hemolysis. The supercooling group exhibits a significantly lower hemolysis rate of 0.76% at day 63 compared to the control group's 0.88% ($p < 0.05$) (Fig. 2C).

To assess metabolic stability, we measured key parameters including glucose consumption, lactate accumulation, pH levels, adenosine triphosphate (ATP), and 2,3-diphosphoglycerate (2,3-DPG) concentrations. The supercooling group maintains significantly higher glucose levels and exhibits lower lactate accumulation compared to the control group, with notable differences at 42 days ($p = 0.002$ for glucose; $p < 0.05$ for lactate) (Fig. 2D-E).

Additionally, the decline in pH is less pronounced in the supercooling group, reaching 6.43 at day 63 versus 6.19 in the control group ($p < 0.05$) (Fig. 2F). ATP levels, essential for RBC functionality, remain significantly higher in the supercooling group (3.06 nmol/mg) compared to the control group (2.17 nmol/mg) at 42 days ($p < 0.05$) (Fig. 2G). The concentration of 2,3-DPG, crucial for oxygen release capacity, shows a markedly slower decline in the supercooling group, with both groups leveling off post 42 days ($p = 0.206$) (Fig. 2H). These results indicate that supercooling preservation effectively decelerates metabolic degradation of RBC, maintaining essential biochemical functions over extended storage durations.

Collectively, these results demonstrate that supercooling preservation at -8 °C significantly minimizes hemolysis and metabolic degradation of RBC. The maintained levels of ATP and 2,3-DPG, indicate that supercooling effectively preserves RBC functionality and viability over prolonged storage periods. Consequently, our supercooling protocol offers a superior preservation method, mitigating the hemolysis and metabolic lesions.

Supercooling preservation reduces oxidative stress and maintains RBC membrane integrity

To evaluate the impact of supercooling preservation on oxidative stress and membrane integrity in RBCs, we conducted a series of biochemical assays and morphological analyses over a 63-day storage period (Fig. 3A). We measured ROS and MDA levels to assess oxidative stress, and evaluated the activities of superoxide dismutase (SOD) and catalase (CAT) to determine the RBCs' antioxidative defense capacity. Additionally, we examined membrane integrity through osmotic fragility tests and phosphatidylserine (PS) exposure, and analyzed RBC morphology using blood smears.

We observed that RBCs preserved under supercooling conditions exhibit significantly lower increases in ROS and MDA levels compared to the control group stored at 4 °C ($p < 0.05$) (Fig. 3B-C). Specifically, ROS levels in the supercooling group rise modestly over time, whereas the control group shows a higher increase, indicating higher oxidative stress in conventional storage. Similarly, MDA concentrations, a marker of lipid peroxidation, remain relatively stable in the supercooling group but increase significantly in the control group, reflecting reduced lipid membrane damage in supercooled RBCs.

Furthermore, the activities of antioxidant enzymes SOD and CAT remain largely stable in the supercooling group throughout the storage period, with only minor decreases observed towards day 63 (Fig. 3D-E). In contrast, the control group exhibits a significant decline in CAT activity by the end of the storage period, suggesting compromised antioxidative defenses. These results indicate that supercooling preservation effectively mitigates oxidative stress, maintaining the antioxidative capacity of RBCs and protecting them from oxidative damage.

To assess membrane integrity, we performed osmotic fragility tests and measured PS exposure on RBC surfaces. The supercooling group demonstrates lower mean cell fragility (MCF) values compared to controls, indicating enhanced membrane stability (Fig. 3F). Flow cytometry analysis revealed significantly reduced PS exposure in the supercooling group at day 63 ($p < 0.05$) (Fig. 3G, S6), suggesting diminished membrane asymmetry disruption and delayed recognition by phagocytes. Morphological assessments using blood smears showed that RBCs in the supercooling group retain their typical elliptical, biconcave shape with minimal formation of sphero-echinocytes and fragmented cells (Fig. 3H, S7). In contrast, control RBCs exhibit pronounced morphological abnormalities, including increased echinocytosis and cell fragmentation, indicative of membrane damage and compromised structural integrity.

These findings demonstrate that supercooling preservation at -8 °C effectively reduces oxidative stress and maintains RBC membrane integrity over extended storage periods. By minimizing ROS and MDA accumulation and preserving antioxidant enzyme activities, our supercooling protocol protects RBCs from oxidative damage. Additionally, the maintenance of membrane integrity and normal morphology in supercooled RBCs underscores the method's efficacy in preserving cellular functionality and viability. Consequently, supercooling presents a superior preservation strategy by mitigating oxidative stress and membrane damage associated with conventional refrigeration, thereby enhancing the overall quality and safety of stored RBCs for transfusion.

Supercooling-preserved rabbit-RBCs exhibit superior *in vivo* transfusion quality

Higher percentages and longer periods of circulating RBC indicate superior RBC quality (Fig. 4A), US and European guidelines dictate an in vivo 24-h post-transfusion survival of at least 75% [3]. To evaluate the clinical viability of supercooling-preserved RBC, we conducted in vivo transfusion studies using New Zealand white rabbits. The self-life of rabbit-RBCs is 50 days, while the self-life of human RBCs is 120 days [57, 58]. Based on this ratio, the recovery rate of supercooling-preserved human RBCs for 63 days is roughly equivalent to that of supercooling-preserved rabbit-RBCs for 28 days. Thus, we assessed the recovery rates of supercooling-preserved rabbit-RBCs for 35 days in vitro compared to conventionally stored controls.

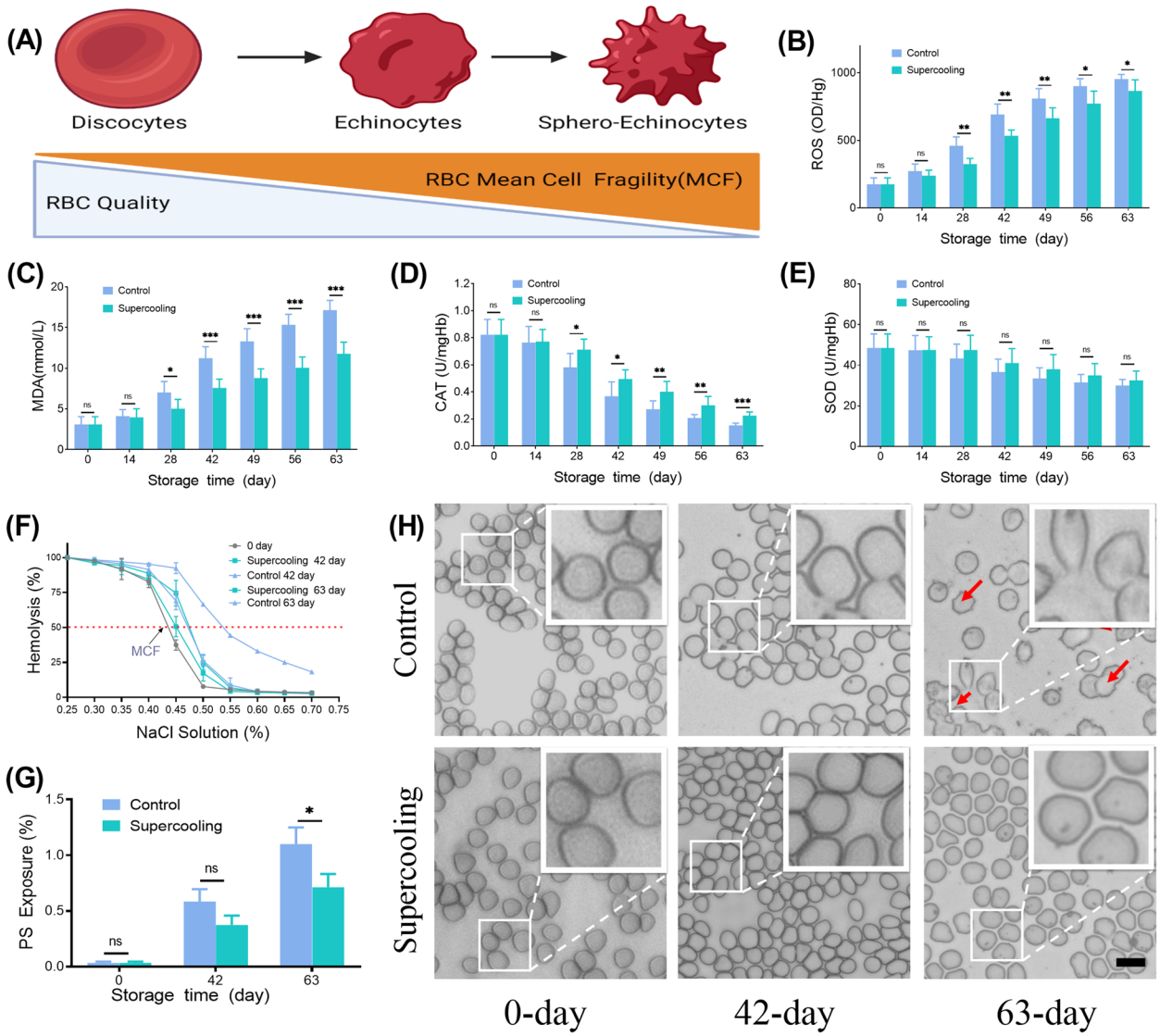

Fig. 3 In vitro analysis oxidative stress and membrane integrity of RBC. **A** Schematic of storage-induced RBC morphologic change. Healthy discocytes into non-healthy echinocytes and sphero-echinocytes. **B-E** Oxidative stress markers: ROS, MDA, SOD, and CAT levels. Mean values of ROS **B**), MDA **C**), CAT **D**), and SOD **E**) in RBC samples at 0, 14, 28, 42, 49, 56, and 63 days. Control (blue) and supercooling (green). Data are shown as the mean ± SD from six biological replicates ($n = 6$). independent samples t-test, $^{*}p < 0.05$; $^{***}p < 0.001$; ns, nonsignificant. **F–H** Membrane integrity and morphological changes: MCF, PS exposure, and RBC morphology. **F**) Mean values of Osmatic fragility test. To characterize RBC membrane integrity, we conducted the osmotic fragility test by resuspending the stored RBCs in a hypotonic solution. Mean cell fragility (MCF) reflects the NaCl concentration at which 50% hemolysis occurs. Data are shown as the mean ± SD from three biological replicates ($n = 3$). **G** PS exposure in the supercooled group was significantly lower than that in the control group (statistical result). Data are shown as the mean ± SD from three biological replicates ($n = 3$). $^{*}p < 0.05$; ns, nonsignificant. **H** Morphological changes in the control group were mainly irreversible at the end of the preservation period. The morphological changes in the supercooled group were mainly reversible at the end of the preservation period. Red arrow: irreversible changes (sphero-echinocytes and fragmented RBCs). Scale bar = 10 μm

We first isolated rabbit-RBCs from rabbit whole blood by centrifugation to remove platelet-poor plasma and buffy coat, followed by resuspension in mannitol–adenine–phosphate (MAP) solution. Rabbit-RBCs were then either stored at 4 °C (control group) or subjected to our supercooling preservation protocol at −8 °C (supercooling group) for varying durations (0, 14, 21, 28 and 35 days). At each storage interval, rabbit-RBCs were labeled with carboxyfluorescein diacetate succinimidyl ester ($CFSE^{+}$) to facilitate tracking post-transfusion. Approximately 4 ml of labeled rabbit-RBCs were transfused into recipient rabbits via the ear vein (Fig. 4B).

Morphological assessments using blood smears revealed that supercooled rabbit-RBCs of rabbit retain their typical elliptical, biconcave shape with minimal morphological abnormalities over time (Fig. 4C), whereas control rabbit-RBCs exhibit increased sphero-echinocyte and fragmented cell formations indicative of membrane damage and reduced deformability. Our nonradioactive flow cytometry method, based on $CFSE^+$ labeling, demonstrated that nearly all transfused rabbit-RBCs are successfully labeled, ensuring accurate tracking of rabbit-RBC survival. The log fluorescence intensity versus cell counts plots confirmed consistent $CFSE^+$ staining across all samples (Fig. 4D, S8). Immediately after transfusion (0-day storage), both supercooling-preserved and control rabbit-RBCs demonstrate high recovery rates, with fresh rabbit-RBCs achieving a 94.83% recovery at 24 h post-transfusion. After 14 days of storage, the control group shows an 82.69% recovery rate, while the supercooling group maintains over 90% recovery. At 21 days, recovery rates declined to 65.26% in the control group and remained robust at 84.09% in the supercooling group, at 28 days, recovery rates of supercooling group still above 75%. Although at 35 days, the supercooling group's recovery rate decreases to 53.01%, it was still significantly higher than the control group's rate (Fig. 4E).

Supercooling-preserved rabbit-RBCs showed a higher persistence of $CFSE^+$ cells in circulation at 24 h post-transfusion compared to control rabbit-RBCs, corroborating the recovery rate data. These findings indicate that supercooling preservation significantly enhances the in vivo transfusion quality of rabbit-RBCs. Supercooled rabbit-RBCs maintained higher recovery rates at critical storage intervals (14, 21 and 28 days), demonstrating superior viability and functionality compared to conventionally stored controls. Although the recovery rate for supercooled rabbit-RBCs decreased below 75% after 35 days of supercooling preservation, it remained markedly higher than that of the control group, highlighting the effectiveness of supercooling in preserving rabbit-RBC quality over extended storage periods. The superior in vivo recovery rates of supercooling-preserved rabbit-RBCs suggest enhanced transfusion outcomes, potentially reducing the risks associated with transfusion of older blood units, such as postoperative complications and increased mortality rates. This advancement underscores the translational potential of our supercooling preservation protocol, offering a viable solution to extend RBC shelf life and improve the safety and efficacy of blood transfusions in clinical settings (Table. S1).

Discussion

Traditional methods for RBC preservation, particularly cryopreservation, offer extended storage durations but are hindered by significant challenges. Cryopreservation necessitates the use of high concentrations of glycerol (> 20%) as cryoprotective agents (CPAs) to maintain RBC viability below −65 °C [23, 25, 27]. However, the addition and subsequent removal of glycerol induce transient osmotic gradients, resulting in cytotoxicity and osmotic injuries that lead to severe hemolysis [21]. Additionally, the deglycerolization process involves multiple washing and centrifugation steps, which can delay emergency transfusions [18, 26, 59, 60]. Alternative preservation methods, such as freeze-drying, offer a promising solution for room-temperature storage of RBC by eliminating the need for ultra-low temperatures. However, this method is still limited by ice crystal formation during the freezing phase, which can cause mechanical damage to cellular membranes and hemoglobin structures [22]. These limitations underscore the urgent need for innovative preservation techniques that can extend RBC shelf life without compromising cellular integrity or clinical utility.

Engineered supercooling protocol enhances stability and scalability for large-volume RBC preservation

Our study introduces an engineered supercooling preservation protocol specifically designed to address the challenges associated with large-volume RBC storage in commercial PVC blood bags. By integrating paraffin oil sealing with precise thermal control mechanisms, we successfully maintained 100 ml of RBC suspensions at

(See figure on next page.)

Fig. 4 In vivo transfusion studies demonstrating post-transfusion RBC recovery rate. **A** During storage, PS expression on the RBC surface can promote RBC adhesion to endothelial cells, leading to RBC clearance by macrophages. Consequently, outer leaflet PS exposure on the RBC membrane acts as an 'eat-me' signal. **B** Overview of the experimental setup for rabbit transfusion studies. Preparation of allogeneic RBC concentrates from donor rabbits and transfusion. New Zealand white rabbits were acquired and subjected to a series of steps for blood collection, centrifugation, and purification. Once prepared, the RBCs were stored under supercooling preservation. Following specific time intervals, RBCs were marked with $CFSE^+$ and transfused back into the rabbits. **C** Morphological analysis of transfused RBC using blood smears. The morphological changes of rabbit RBC in control group and supercooling group with storage time. Red arrow: irreversible changes (sphero-echinocytes and fragmented RBCs). Scale bar = 10 μm. **D** Flow cytometry plots showing $CFSE^+$ RBC labeling. **E** Recovery rates of RBCs stored at 4 °C versus supercooling conditions over 35 days. RBCs recovery in vivo after transfusion 24 h of supercooling preserve and control preserve on the 0, 14, 21, 28 and 35 days. Data are shown as the mean ± SD from three biological replicates ($n = 3$). independent samples t-test, $^*p < 0.05$; ns, nonsignificant

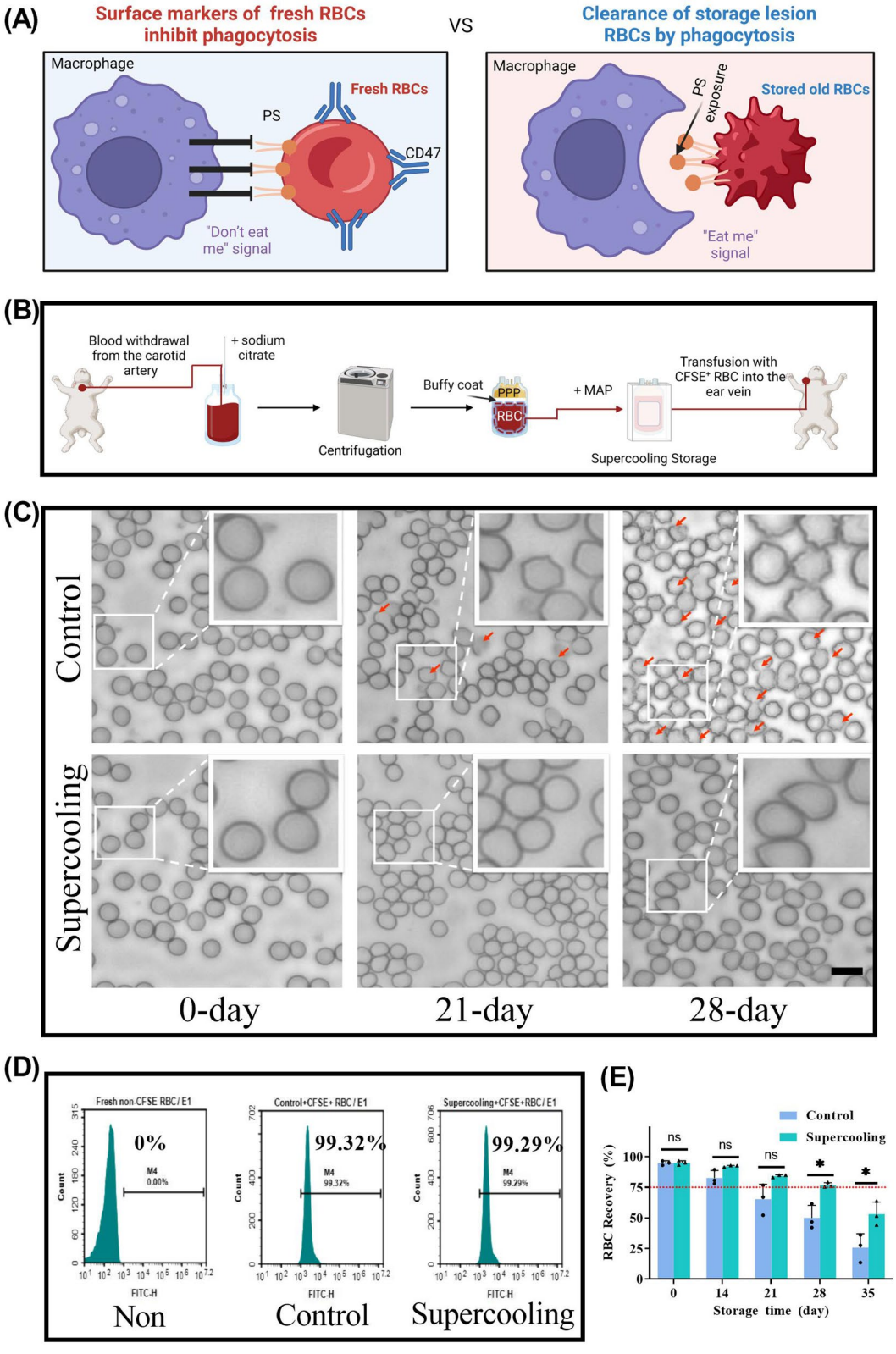

Fig. 4 (See legend on previous page.)

–8 °C for up to 63 days (Fig. 1A). The use of paraffin oil effectively eliminates heterogeneous nucleation at the liquid–air interface, a critical factor in preventing ice crystal formation in the metastable supercooled state [40]. Additionally, adhering the flexible PVC blood bags to rigid baseplates using double-sided tape minimized deformation and ensured the stability of the oil seal during storage, a key innovation that differentiates our protocol from previous approaches [38–40, 45, 61]. The orthogonal experimental design optimized six critical factors (storage temperature, RBC volume, placement angle, cooling rate, baseplate material, and sealing oil volume), resulting in enhanced supercooling stability with minimal freezing events (Table 2).

Although hypothermic storage (4 °C) and cryopreservation are widely utilized for RBC preservation, both approaches exhibit critical limitations that may compromise transfusion efficacy and safety. For hypothermic storage, the restricted shelf life (typically ≤ 42 days) is accompanied by a progressive decline in RBC quality. In contrast, cryopreservation extends storage duration to years but introduces technical and biological challenges [17]. One recent advance is the preservation of RBCs at -8.0 °C for an impressive 70 days without freezing by adding a low concentration of glycerol combined with PEG-400 to reduce the freezing point. However, given the tedious rewarming and washing processes and very small storage volume (5 ml), its clinical practicality remains limited [23]. Our engineering strategy not only ensures the reliability and reproducibility of the supercooling state in large-volume suspensions in commercial blood bags but also highlights the scalability and practicality of our preservation system for clinical applications (Fig. 5).

Supercooling mitigates metabolic and oxidative stress, preserving RBC functionality

Supercooling preservation significantly mitigates metabolic and oxidative stress of RBC, thereby maintaining cellular functionality and viability over extended storage periods. Our results demonstrate that supercooled RBCs exhibit reduced hemolysis (0.76% in supercooling vs 0.88% in controls after 63 days) and maintain higher levels of essential metabolic markers such as glucose, ATP, and 2,3-DPG compared to conventionally stored RBCs. The slower glycolysis rate in supercooled RBCs leads to delayed lactate accumulation and less pronounced pH drops, indicating a deceleration of metabolic degradation [4]. Oxidative stress was an important mechanism of injury at subzero temperatures. Blood bags, optimize oxygen and nutrient exchange due to gas-permeable surfaces, provide a more controlled oxygen environment. In addition, the choice of an appropriate additive solution (AS) for RBC is crucial for supercooling preservation at low temperatures [39]. In this study, we selected the latest and most comprehensive formulation of MAP solution as the AS for RBC storage. Compared to the other AS, the RBC stored in MAP solution experienced lower hemolysis and ensured continued glycolytic activity during supercooling preservation, primarily due to its multifaceted mechanisms in mitigating oxidative damage, stabilizing metabolic homeostasis. For example, mannitol scavenges oxygen radical via its hydroxyl groups and optimizes antioxidant capacity through the citrate–phosphate buffer system, directly attenuating oxidative stress on membrane lipids and hemoglobin [5]. By maintaining metabolic homeostasis and reducing oxidative insults, supercooling preservation preserves RBC membrane integrity and prevents morphological transformations, such as echinocytosis and cell fragmentation. These biochemical and structural protections collectively enhance the overall quality and functionality of RBCs, ensuring their efficacy for transfusion purposes.

Supercooling-preserved RBC demonstrate superior transfusion outcomes with clinical potential

The ultimate test of RBC preservation efficacy lies in their performance during transfusion. Our in vivo studies using New Zealand white rabbits demonstrate that supercooling-preserved RBCs exhibit superior post-transfusion recovery rates compared to conventionally stored controls. Following storage for 28 days, supercooled RBCs maintained recovery rates exceeding 75%, significantly outperforming the control group, which showed recovery rates of 50.13%, respectively. Although recovery rates for supercooled RBCs declined to 53.01% at 35 days, this still represented a substantial improvement over the control group (25.69%) and highlighted the potential for further optimization to meet FDA guidelines for successful transfusions [62]. Morphological analyses confirmed that supercooled RBCs retained their typical elliptical, biconcave shape with minimal morphological abnormalities, enhancing their deformability and microcirculatory function. Flow cytometry using $CFSE^+$ labeling verified the higher persistence of supercooled RBCs in circulation post-transfusion, affirming their enhanced viability and functionality. These findings suggest that supercooling preservation not only extends the shelf life of RBCs but also ensures their clinical efficacy, reducing the risks associated with transfusion of older blood units and improving patient outcomes.

Clinical implications and future directions

Our engineered supercooling preservation protocol offers a transformative solution to the longstanding challenges in RBC storage and transfusion medicine. By significantly reducing hemolysis, metabolic degradation,

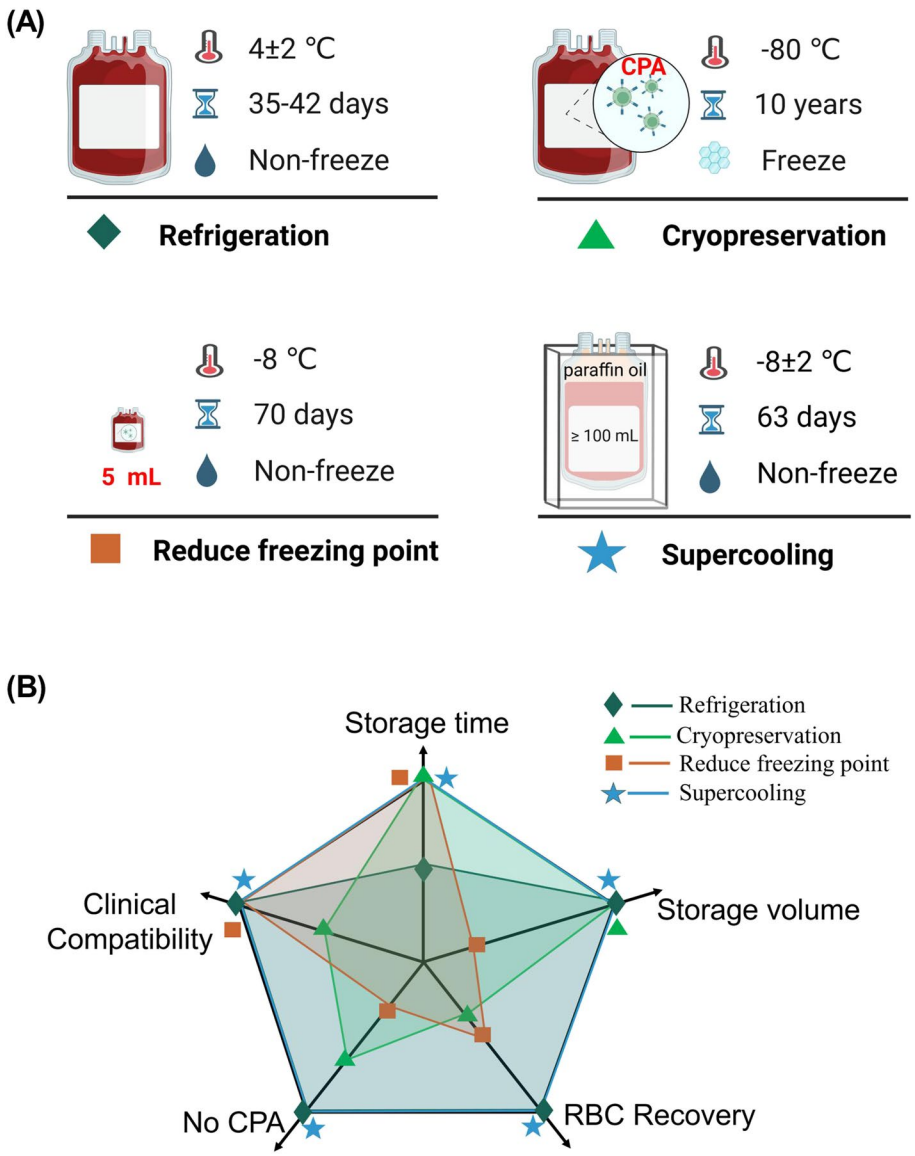

Fig. 5 **A** Different RBC preservation method and characteristic. **B** Supercooling preserve storage time is longer, the volume is larger, the clinical compatibility is relatively good, higher RBC recovery, no additional cryoprotectant and no additional washing processes

and oxidative stress, supercooling maintains RBC integrity and functionality, thereby enhancing transfusion safety and efficacy. The scalability and compatibility of our system with existing blood banking infrastructure facilitate its potential for widespread clinical adoption. Volumes of RBC concentrates prepared from 450 to 500 ml donations are suitable for clinical needs in many countries. In China, there are three types of whole blood donation volume: 200 ml, 300 ml and 400 ml, and the corresponding volume of leukocyte-reduced red blood cells can be prepared as about 170 ml, 250 ml and 360 ml after adding an additive solution. Besides, smaller volumes of red blood cells such as 100 ml and 50 ml or even less are commonly used in neonates and infant transfusion. Therefore, 100 ml of RBCs can represent a clinically relevant volume.

Our study has two primary limitations. First, the supercooling preservation shelf-life of hRBC remains suboptimal. Future research should focus on further optimizing the supercooling protocol to extend RBC shelf life beyond 63 days. For example, an automated oil-sealing system is proposed to replace the manual oil-sealing process, which further reduces ice nucleation risks and enables large-volume hRBCs to achieve stable

supercooling at temperatures below -8 °C. Second, we did not test the recovery rate of supercooled hRBCs in humans. Clinical trials are essential to validate the safety and efficacy of supercooling-preserved RBCs in human transfusions, paving the way for regulatory approval and routine clinical use. Additionally, investigating the integration of novel additive solutions and conducting large-scale metabolomic and proteomic analyses could provide deeper insights into the mechanisms underlying RBC preservation and identify targets for further enhancement [63].

Conclusions

In summary, we present an engineered supercooling preservation system that extends the shelf life of large-volume (100 ml) red blood cell suspensions in commercial PVC blood bags. By integrating paraffin oil sealing with precise thermal control at −8 °C, our protocol minimizes hemolysis, metabolic degradation, and oxidative stress, while preserving RBC membrane integrity and functionality for up to 63 days. In vivo transfusion studies using New Zealand white rabbits demonstrate that supercooling-preserved RBCs achieve superior post-transfusion recovery rates compared to conventionally stored controls, underscoring the clinical viability and enhanced transfusion quality of our method.

Materials and methods

Ethical approval

This study was approved by the Ethics Committee of the First Affiliated Hospital of Army Medical University, PLA (Approval Number: (A) KY2021071). All experiments were conducted in accordance with ethical standards. RBC samples were obtained from healthy donors at the Department of Blood Transfusion, First Affiliated Hospital of Army Medical University, Chongqing, China.

Optimization of supercooling conditions

To identify optimal conditions for supercooling preservation, we conducted an orthogonal experimental design considering six key factors: storage temperature, RBC volume, placement angle, cooling rate, baseplate material, and sealing oil volume (Table 1, Fig. S1). Each factor was tested at three levels, resulting in 18 experimental combinations. The primary outcome was freezing frequency, defined as the ratio of frozen samples to total samples. Data were analyzed using SPSS 22.0, applying Arcsine Transformation to normalize the freezing frequency results.

Supercooling preservation protocol

We developed an engineered supercooling preservation system using commercial PVC blood bags. Each blood bag was securely affixed to a rigid baseplate using double-sided tape to prevent deformation during storage. For the supercooling groups, 100 ml of RBC suspension was transferred into the sealed PVC blood bag and topped with 8 ml of paraffin oil (Sigma-Aldrich, USA) to minimize ice nucleation (Fig. S2). The sealed bags were then stored at -8 °C in a temperature-controlled refrigerator (BD-168WGHECD; Haier, China). Control samples were stored at 4 °C in a separate refrigerator (BCD-628WACW; Haier, China). Temperature fluctuations were minimized using different baseplate materials (copper, glass, styrofoam) to evaluate their effect on supercooling stability. Temperature stability was monitored continuously using T-type thermocouples attached to the surface of each blood bag.

Detection of freezing events

Freezing events were identified through direct visual inspection and mechanical testing. Blood bags were tilted to assess flow and deformation; frozen samples remained static upon tilting, whereas supercooled samples maintained fluidity. Successful supercooling was confirmed by transparency and lucidity of the RBC suspension, indicative of the absence of ice crystals (Fig. S9). Stability tests were documented in Supplementary Movie S1.

Sample preparation and storage

Two units RBC was prepared from 400 ml whole blood, and the total volume was about 360 ± 10% ml after adding MAP (100 ml MAP contained the following components: mannitol 1.457 g, glucose 0.793 g, sodium chloride 0.497 g, sodium citrate 0.15 g, sodium dihydrogen phosphate 0.094 g, citric acid 0.02 g, adenine 0.014 g). In our experiments, RBCs were first supplemented with 10–15 ml MAP to·400 ml and subsequently divided into four equal aliquots using standardized commercial blood bags, one aliquot served as the control group (stored at 4 °C), while the remaining three aliquots comprised the supercooling group (preserved at −8 °C with paraffin oil sealing and rigid baseplate stabilization). Each aliquot was exclusively allocated to a single timepoint analysis, 6 aliquots from two 400 ml RBCs provided sufficient sample to conduct all scheduled time-point assessments for the supercooling group (14, 28, 42, 49, 56, and 63 days). To ensure statistical power, a total of 12 × 400 ml RBCs were divided and analyzed, enabling six biological replicates per timepoint. The blood bags for each aliquot RBCs in this study had dimensions of 140 mm (length) × 80 mm (width) with a single-layer wall thickness of 0.4 mm (Supplier: Nigale Biomedical Co., Ltd., China, No. 201221).

In Vitro analysis of RBC preservation

Hemolysis assessment

Hemolysis was quantified by centrifuging RBC samples at 3,000 rpm for 10 min. The supernatant was diluted with Tris–HCl (pH 8.0) and measured spectrophotometrically at 380 nm, 415 nm, and 450 nm using a microplate reader (Thermo Fisher Scientific, Finland). The Hb and HCT were measured by the hematocytometer (XS-900i; Sysmex, Japan). Free hemoglobin (F-Hb) was calculated using the formula: F-Hb(g/L) = (2OD415–OD380–OD450) × 0.84 [64]. Hemolysis percentage was determined as Hemolysis (%) = F-Hb × (1 – HCT) / Hb × 100.

Metabolic and oxidative stress analysis

Metabolic and oxidative stress parameters including pH, glucose, lactate, ATP, 2,3-DPG, ROS, MDA, SOD, and CAT. The pH was detected using a pH meter (PB-21; Sartorius, Germany), ATP was measured by the Enhanced ATP Assay Kit (S0027; Beyotime, China); 2,3-DPG was detected by the Human 2,3-Disphosphoglycerate ELISA Kit (JL10440; Jiang Lai, China); glucose was detected by the Glucose Assay Kit with O-toluidine Method (S0201S; Beyotime, China), and lactate was detected by the Human LAC ELISA Kit (JL19760; Jiang Lai, China). Reactive oxygen species levels were evaluated with the ROS Assay Kit (S0033S; Beyotime, China), and malondialdehyde was quantified using the lipid peroxidation MDA assay kit (S0131S; Beyotime, China). Antioxidant enzymes superoxide dismutase and catalase were measured using respective determination kits (S0101S; Beyotime, China; A007; Jiancheng, China). All assays were performed according to manufacturer protocols.

Membrane integrity and morphological analysis

Membrane damage was assessed by measuring mean cell fragility (MCF) through osmotic fragility tests. RBC suspensions were exposed to varying NaCl concentrations (0.25% to 0.70%) and hemolysis was quantified by measuring the optical density at 540 nm. Phosphatidylserine exposure was analyzed using Annexin V-FITC (C1062M; Beyotime, China) staining followed by flow cytometry (BD Biosciences, CA). Morphological changes were evaluated via blood smears observed under an inverted microscope at 600 × magnification (Olympus IX53, Japan), categorizing irreversible RBCs as sphero-echinocytes and fragmented cells.

In vivo transfusion studies

New Zealand white rabbits (3.0 ± 0.5 kg, male) were anesthetized with intramuscular injections of pentobarbital (30 mg/kg). About 100 ml of blood samples were collected aseptically into sodium citrate-containing blood bags via the carotid artery and processed to isolate RBCs by centrifugation (3600 g for 10 min at 4 °C remove platelet-poor-plasma and buffy coat). Purified RBCs were resuspended in MAP solution and stored either at 4 °C or using the supercooling protocol at -8 °C as described above [65].

At designated storage intervals, RBCs were labeled with carboxyfluorescein diacetate succinimidyl ester (CFSE; abs9106; absin), then washed twice in MAP to remove excess fluorescent dye, and transfused (4 ml) into the ear vein of recipient rabbits. RBC recovery was assessed at 5 min and 24 h post-transfusion using flow cytometry, calculating recovery rates as (%$CFSE^+$ RBCs at 24 h / %$CFSE^+$ RBCs at 5 min) × 100 [62]. All animal experiments complied with the Laboratory Animal Welfare and Ethics Committee of Third Military Medical University guidelines (Approval Number: AMUWEC20210333).

Statistical analysis

Data were first assessed for normality using the Shapiro–Wilk test. Comparisons between groups were performed using Student's two-tailed t-test with the assumption of equal variances, implemented in SPSS 22.0. Data are presented as mean ± standard deviation, with statistical significance set at $p < 0.05$. Specific sample sizes for each analysis are detailed in the corresponding figure legends.

Supplementary Information

The online version contains supplementary material available at https://doi.org/10.1186/s13036-025-00510-2.

Supplementary Material 1. Additional experimental details, including orthogonal experiment tables (Table S1), supplementary figures (Figs. S1-S10), and a demonstration movie (Movie S1), are provided in the supplementary materials.

Acknowledgements

We thank Shangsheng Feng, and Pengpeng Jia of Xi'an Jiaotong University for input, discussions and heat transfer technical assistance.

Authors' contributions

Q. Liu, S.C. Wang, C.Y. Yao and F. Xu conceived and designed the study. Q. Liu, S.C. Wang, C.Y. Yao and F. Xu wrote the manuscript and extensively edited the manuscript. Q. Liu and R. H. Diao collected the blood samples. Q. Liu performed experiments. Q. Liu, S.C. Wang and H.S. Huang analyzed the data. Q. Liu and J. Yan made the graphs to visualize the data. C.Y. Yao and S.C. Wang provided resources and support.

Funding

The research was supported by the National Natural Science Foundation of China (No. 82470235, 21904104), the Natural Science Foundation of Chongqing, China (No. CSTC2021JCYJ-MSXMX0702), the National Key Research and Development Program of China (No. 2016YFC0101300) and the Shaanxi Sanqin Scholars Innovation Team Support Plan (No. XTR062021001).

Data availability

No datasets were generated or analysed during the current study.

Declarations

Ethics approval and consent to participate

All participants were over 18 years old and provided written informed consent for sample collection and analysis. The research procedure was approved by the Ethics Committee of the First Affiliated Hospital of Army Medical University, PLA (Approval Number: (A) KY2021071). All animal experiments complied with the Laboratory Animal Welfare and Ethics Committee of Third Military Medical University guidelines (Approval Number: AMUWEC20210333).

Consent for publication

All authors have seen and approved the final version of the paper, and all are aware of the submission of the paper.

Competing interests

The authors declare no competing interests.

Received: 29 March 2025 Accepted: 16 April 2025
Published online: 06 May 2025

References

1. Shafique MA, et al. Transfusion strategies for neonates: current perspectives. Ann Med Surg (Lond). 2024;86(3):1550–62.
2. Neal MD, Hunt BJ. Precision in Transfusion Medicine. JAMA. 2023;330(19):1847–8.
3. Carson JL, et al. Red Blood Cell Transfusion: 2023 AABB International Guidelines. JAMA. 2023;330(19):1892–902.
4. Hess JR. RBC storage lesions. Blood. 2016;128(12):1544–5.
5. D'Alessandro A, Liumbruno G, Grazzini G, Zolla L. Red blood cell storage: the story so far. Blood Transfus. 2010;8(2):82–8.
6. Yoshida T, Prudent M, D'Alessandro A. Red blood cell storage lesion: causes and potential clinical consequences. Blood Transfus. 2019;17(1):27–52.
7. Williamson LM, Devine DV. Challenges in the management of the blood supply. Lancet. 2013;381(9880):1866–75.
8. Lagerberg JW, Korsten H, Van Der Meer PF, De Korte D. Prevention of red cell storage lesion: a comparison of five different additive solutions. Blood Transfus. 2017;15(5):456–62.
9. Walker WH, Netz M, Ganshirt KH. 49 day storage of erythrocyte concentrates in blood bags with the PAGGS-mannitol solution. Beitr Infusionsther. 1990;26:55–9.
10. T. Nemkov et al., Supercooled storage of red blood cells slows down the metabolic storage lesion. Res Sq. 2025.
11. Qin X, et al. Core-Shell Microfiber Encapsulation Enables Glycerol-Free Cryopreservation of RBCs with High Hematocrit. Nanomicro Lett. 2023;16(1):3.
12. J. Xu, C. Lei, W. Zhu, Nanomaterial-Enhanced Red Blood Cell Biopreservation: From Refrigeration to Cryopreservation. Chembiochem. 2024, e202400827.
13. Kim E, Park S, Hwang S, Moon I, Javidi B. Deep Learning-Based Phenotypic Assessment of Red Cell Storage Lesions for Safe Transfusions. IEEE J Biomed Health Inform. 2022;26(3):1318–28.
14. Doan M, et al. Objective assessment of stored blood quality by deep learning. Proc Natl Acad Sci U S A. 2020;117(35):21381–90.
15. P. Bruun-Rasmussen, P. Kragh Andersen, K. Banasik, S. Brunak, P. I. Johansson, Intervening on the storage time of RBC units and its effects on adverse recipient outcomes using real-world data. Blood. 2022; 139(25), 3647–3654.
16. Rabcuka J, et al. Metabolic reprogramming under hypoxic storage preserves faster oxygen unloading from stored red blood cells. Blood Adv. 2022;6(18):5415–28.
17. D'Alessandro A, Hod EA. Red Blood Cell Storage: From Genome to Exposome Towards Personalized Transfusion Medicine. Transfus Med Rev. 2023;37(4): 150750.
18. Jang TH, et al. Cryopreservation and its clinical applications. Integr Med Res. 2017;6(1):12–8.
19. Shen L, et al. Fine-tuned dehydration by trehalose enables the cryopreservation of RBCs with unusually low concentrations of glycerol. Journal of Materials Chemistry B. 2021;9(2):295–306.
20. Lin M, Cao H, Li J. Control strategies of ice nucleation, growth, and recrystallization for cryopreservation. Acta Biomater. 2023;155:35–56.
21. Sun Y, et al. Ice Recrystallization Inhibition Is Insufficient to Explain Cryopreservation Abilities of Antifreeze Proteins. Biomacromol. 2022;23(3):1214–20.
22. T. Chakkumpulakkal Puthan Veettil *et al.*, Characterization of freeze-dried oxidized human red blood cells for pre-transfusion testing by synchrotron FTIR microspectroscopy live-cell analysis. Analyst. 2023; 148(7), 1595–1602.
23. Zhu C, Niu Q, Yuan X, Chong J, Ren L. NonFreezable Preservation of Human Red Blood Cells at -8 degrees C. ACS Biomater Sci Eng. 2022;8(6):2644–53.
24. Nemkov T, Yoshida T, Nikulina M, D'Alessandro A. High-Throughput Metabolomics Platform for the Rapid Data-Driven Development of Novel Additive Solutions for Blood Storage. Front Physiol. 2022;13: 833242.
25. Murray A, Congdon TR, Tomas RMF, Kilbride P, Gibson MI. Red Blood Cell Cryopreservation with Minimal Post-Thaw Lysis Enabled by a Synergistic Combination of a Cryoprotecting Polyampholyte with DMSO/Trehalose. Biomacromol. 2022;23(2):467–77.
26. Liu Y, et al. A 3D-printed transfusion platform reveals beneficial effects of normoglycemic erythrocyte storage solutions and a novel rejuvenating solution. Lab Chip. 2022;22(7):1310–20.
27. X. Liu et al., Tricine as a Novel Cryoprotectant with Osmotic Regulation, Ice Recrystallization Inhibition and Antioxidant Properties for Cryopreservation of Red Blood Cells. Int J Mol Sci. 2022; 23(15).
28. Kim CY, et al. Deuterated Linoleic Acid Attenuates the RBC Storage Lesion in a Mouse Model of Poor RBC Storage. Front Physiol. 2022;13: 868578.
29. de Bruin S, et al. Storage of red blood cells in alkaline PAGGGM improves metabolism but has no effect on recovery after transfusion. Blood Adv. 2022;6(13):3899–910.
30. Finger EB, Bischof JC. Cryopreservation by vitrification: a promising approach for transplant organ banking. Curr Opin Organ Transplant. 2018;23(3):353–60.
31. N. Manuchehrabadi *et al.*, Improved tissue cryopreservation using inductive heating of magnetic nanoparticles. Sci Transl Med. 2017; 9(379).
32. Zhao Y, Lou L, Lyu C, Powell-Palm MJ, Rubinsky B. Isochoric supercooling cryomicroscopy. Cryobiology. 2022;106:139–47.
33. D. H. Park, E. J. Kim, H. Kim, G. P. Hong, M. J. Choi, Conditions of the Stepwise Cooling Algorithm for Stable Supercooling Preservation and Freshness of Pork Loin. Foods. 2022; 11(24).
34. Dou M, Lu C, Rao W. Bioinspired materials and technology for advanced cryopreservation. Trends Biotechnol. 2022;40(1):93–106.
35. D. Zemmyo, M. Yamamoto, S. Miyata, Efficient Decellularization by Application of Moderate High Hydrostatic Pressure with Supercooling Pretreatment. Micromachines (Basel). 2021; 12(12).
36. Y. You et al., Application of Supercooling for the Enhanced Shelf Life of Asparagus (Asparagus officinalis L.). Foods. 2021; 10(10).
37. Kim MY, Yoon HY, Lee S. The Advantage of the Supercooling Storage Method for Transplantable Sources: Human Umbilical Vessel Endothelial Cells and Mouse Skin Grafts. Transplant Proc. 2021;53(5):1756–61.
38. William N, et al. Comparing two extracellular additives to facilitate extended storage of red blood cells in a supercooled state. Front Physiol. 2023;14:1165330.
39. Isiksacan Z, et al. Extended supercooled storage of red blood cells. Commun Biol. 2024;7(1):765.
40. Huang H, Yarmush ML, Usta OB. Long-term deep-supercooling of large-volume water and red cell suspensions via surface sealing with immiscible liquids. Nat Commun. 2018;9(1):3201.
41. de Vries RJ, et al. Supercooling extends preservation time of human livers. Nat Biotechnol. 2019;37(10):1131–6.
42. Huang H, Rey-Bedon C, Yarmush ML, Usta OB. Deep-supercooling for extended preservation of adipose-derived stem cells. Cryobiology. 2020;92:67–75.
43. Danilova E, Ezligini F, Stockel C, Asakawa M, Hetland G. An evaluation of diethylhexyl phthalate free top & bottom in-line blood collection set with a new soft housing filter. Transfus Med. 2025;35(1):82–90.

44. Gulliksson H, Meinke S, Ravizza A, Larsson L, Hoglund P. Storage of red blood cells in a novel polyolefin blood container: a pilot in vitro study. Vox Sang. 2017;112(1):33–9.
45. H. Al Salloum et al., Characterization of the surface physico-chemistry of plasticized PVC used in blood bag and infusion tubing. Mater Sci Eng C Mater Biol Appl. 2017; 75, 317–334.
46. Larsson L, et al. Non-phthalate plasticizer DEHT preserves adequate blood component quality during storage in PVC blood bags. Vox Sang. 2021;116(1):60–70.
47. M. J. Powell-Palm, A. Koh-Bell, B. Rubinsky, Isochoric conditions enhance stability of metastable supercooled water. Applied Physics Letters. 2020; 116(12).
48. Odendahl NL, Geissler PL. Local Ice-like Structure at the Liquid Water Surface. J Am Chem Soc. 2022;144(25):11178–88.
49. Graminske S, et al. In vitro evaluation of di(2-ethylhexyl)terephthalate-plasticized polyvinyl chloride blood bags for red blood cell storage in AS-1 and PAGGSM additive solutions. Transfusion. 2018;58(5):1100–7.
50. Kim J, et al. Supercooling as a potentially improved storage option for commercial kimchi. J Food Sci. 2021;86(3):749–61.
51. Endoh K, Fujikawa S. Mechanism of freezing resistance in eco-dormant birch buds under winter subzero temperatures. Tree Physiol. 2021;41(4):606–18.
52. Vins V, et al. Possible Anomaly in the Surface Tension of Supercooled Water: New Experiments at Extreme Supercooling down to -31.4 degrees C. J Phys Chem Lett. 2020;11(11):4443–7.
53. H. X. Que W, Fujino M, Terayama H, Sakabe K, Fukunishi N, Zhu P, Yi SQ, Yamada Y, Zhong L, Li XK, Prolonged Cold Ischemia Time in Mouse Heart Transplantation Using Supercooling Preservation. Transplantation. 2020; 104(9), 1879–1889.
54. de Vries RJ, et al. Subzero non-frozen preservation of human livers in the supercooled state. Nat Protoc. 2020;15(6):2024–40.
55. Neuner G, Kreische B, Kaplenig D, Monitzer K, Miller R. Deep supercooling enabled by surface impregnation with lipophilic substances explains the survival of overwintering buds at extreme freezing. Plant Cell Environ. 2019;42(7):2065–74.
56. Islamzada E, et al. Blood unit segments accurately represent the biophysical properties of red blood cells in blood bags but not hemolysis. Transfusion. 2022;62(2):448–56.
57. Smith GN, Mollison PL. Normal red cell survival in the rabbit. Scand J Haematol. 1973;11(3):188–94.
58. Pandey S, et al. Intermittent scavenging of storage lesion from stored red blood cells by electrospun nanofibrous sheets enhances their quality and shelf-life. Nat Commun. 2022;13(1):7394.
59. Lin M, Cao H, Meng Q, Li J, Jiang P. Insights into the crystallization and vitrification of cryopreserved cells. Cryobiology. 2022;106:13–23.
60. Chang T, Zhao G. Ice Inhibition for Cryopreservation: Materials, Strategies, and Challenges. Adv Sci (Weinh). 2021;8(6):2002425.
61. S. S. Murthe, S. Sreekantan, R. Mydin, Study on the Physical, Thermal and Mechanical Properties of SEBS/PP (Styrene-Ethylene-Butylene-Styrene/Polypropylene) Blend as a Medical Fluid Bag. Polymers (Basel). 2022; 14(16).
62. Roussel C, et al. Rapid clearance of storage-induced microerythrocytes alters transfusion recovery. Blood. 2021;137(17):2285–98.
63. A. Arav, Cryopreservation by Directional Freezing and Vitrification Focusing on Large Tissues and Organs. Cells. 2022; 11(7).
64. Meng Q, et al. Hypoxic storage of erythrocytes slows down storage lesions and prolongs shelf-life. J Cell Physiol. 2019;234(12):22833–44.
65. Hagisawa K, et al. Efficacy of Resuscitative Transfusion With Hemoglobin Vesicles in the Treatment of Massive Hemorrhage in Rabbits With Thrombocytopenic Coagulopathy and Its Effect on Hemostasis by Platelet Transfusion. Shock. 2018;50(3):324–30.

Publisher's Note